

Antifailure Therapy Including Spironolactone Improves Left Ventricular Energy Supply-Demand Relations in Nonischemic Dilated Cardiomyopathy

Susan P. Bell, MBBS, MSCI; Douglas W. Adkisson, MD; Mark A. Lawson, MD; Li Wang, MS; Henry Ooi, MD; Douglas B. Sawyer, MD, PhD; Marvin W. Kronenberg, MD

Background—Left ventricular (LV) energy supply-demand imbalance is postulated to cause “energy starvation” and contribute to heart failure (HF) in nonischemic dilated cardiomyopathy (NIDCM). Using cardiac magnetic resonance (CMR) and [^{11}C] acetate positron emission tomography (PET), we evaluated LV perfusion and oxidative metabolism in NIDCM and the effects of spironolactone on LV supply-demand relations.

Methods and Results—Twelve patients with NIDCM underwent CMR and PET at baseline and after ≥ 6 months of spironolactone therapy added to a standard HF regimen. The myocardial perfusion reserve index (MPRI) was calculated after gadolinium injection during adenosine, as compared to rest. The monoexponential clearance rate of [^{11}C] acetate (k_{mono}) was used to calculate the work metabolic index (WMI), an index of LV mechanical efficiency, and $k_{\text{mono}}/\text{RPP}$ (rate-pressure product), an index of energy supply/demand. At baseline, the subendocardium was hypoperfused versus the subepicardium (median MPRI, 1.63 vs. 1.80; $P < 0.001$), but improved to 1.80 ($P < 0.001$) after spironolactone. The WMI increased ($P = 0.001$), as did $k_{\text{mono}}/\text{RPP}$ ($P = 0.003$). These improvements were associated with reverse remodeling, increased LV ejection fraction, and decreases in LV mass and systolic wall stress (all $P < 0.002$).

Conclusions—NIDCM is associated with subendocardial hypoperfusion and impaired myocardial oxidative metabolism, consistent with energy starvation. Antifailure therapy improves parameters of energy starvation and is associated with augmented LV performance.

Clinical Trial Registration—URL: <http://www.clinicaltrials.gov/> Unique identifier: ID NCT00574119. (*J Am Heart Assoc.* 2014;3:e000883 doi: 10.1161/JAHA.114.000883)

Key Words: Energy metabolism • heart failure • magnetic resonance imaging • myocardial perfusion imaging • positron emission tomography

A supply-demand energy imbalance, termed myocardial “energy starvation,” may contribute to the pathophysiology of congestive heart failure (HF) which has significant

mortality.^{1–3} Left ventricular (LV) hypertrophy (LVH), hemodynamic overload, and increased wall stress (WS)⁴ lead to increased energy demand, whereas decreased capillary density⁵ may reduce substrate supply. These factors may produce excess energy demand, compared to supply, with adverse metabolic consequences.^{2,6–8}

Methods for quantifying subendocardial perfusion and LV oxidative metabolism make it possible to evaluate energy starvation in patients with nonischemic dilated cardiomyopathy (NIDCM). Decreased transmural hyperemic flow is observed with positron emission tomography (PET) in patients with NIDCM,^{9–11} but cardiac magnetic resonance (CMR) imaging has the spatial resolution to quantitate subendocardial perfusion.^{12–15} The rate of [^{11}C] acetate monoexponential decay using PET imaging (k_{mono}) correlates closely with energy supply denoted by myocardial oxygen consumption,^{16–20} and this method has shown an imbalance of energy supply versus demand in NIDCM,²¹ with reduced LV pump efficiency.^{16,22}

From the Division of Cardiovascular Medicine, Vanderbilt University School of Medicine (S.P.B., D.W.A., M.A.L., H.O., D.B.S., M.W.K.) and Cardiology Section (H.O., M.W.K.), VA Tennessee Valley Healthcare System, Nashville, TN; Department of Biostatistics, Vanderbilt University Medical Center, Nashville, TN (L.W.).

Accompanying Video S1 is available at <http://jaha.ahajournals.org/content/3/4/e000883/suppl/DC1>

Correspondence to: Marvin W. Kronenberg, MD, Vanderbilt Heart and Vascular Institute, Vanderbilt Medical Center East, Suite 5209, 1215 21st Ave, South, Nashville, TN 37232. E-mail: marvin.w.kronenberg@vanderbilt.edu
Received February 12, 2014; accepted August 4, 2014.

© 2014 The Authors. Published on behalf of the American Heart Association, Inc., by Wiley Blackwell. This is an open access article under the terms of the Creative Commons Attribution-NonCommercial License, which permits use, distribution and reproduction in any medium, provided the original work is properly cited and is not used for commercial purposes.

Aldosterone affects the pathophysiology of HF by producing cardiac fibroblast growth and collagen accumulation,^{23–25} marked perivascular fibrosis, endothelial dysfunction, LVH,^{23,26} and reducing large artery compliance.²⁷ Blockade of aldosterone *reduced* mortality from HF in several clinical trials of patients with ischemic and NIDCM.^{28–31}

With a possible reduction of perivascular fibrosis, myocardial perfusion may improve with attendant metabolic and hemodynamic benefits. We employed CMR and PET to assess the hypothesis that long-term aldosterone blockade plus standard HF therapy in patients with NIDCM would improve parameters of energy starvation, including subendocardial perfusion reserve, oxidative metabolism, and LV pump efficiency.

Methods

Study Design and Participants

Twelve patients diagnosed with NIDCM were recruited from the Vanderbilt University Medical Center (Nashville, TN) and the Nashville Veterans Affairs Medical Center (Nashville, TN) from 2008 to 2010 after screening approximately 250 HF patient records. Eligible participants were 18 to 80 years old, of any ethnic background and either sex, and New York Heart Association functional class II to IV HF, with a clinically indicated echocardiogram that measured LV ejection fraction (LVEF) of $\leq 35\%$ and serum potassium level less than 5.0 while on standard therapy for HF, including stable beta-adrenergic blockade and an angiotensin converting-enzyme inhibitor (ACE-I) or angiotensin receptor blocking (ARB) drug for ≥ 3 months. Exclusion criteria were potentially reversible causes of HF, such as myocarditis and peripartum cardiomyopathy, need for an implantable cardioverter-defibrillator, myocardial infarction on electrocardiogram (ECG), a positive stress test or angiographic coronary artery stenosis $\geq 50\%$ in a major artery, severe chronic obstructive airway disease precluding adenosine use, creatinine > 2.5 mg/dL, glomerular filtration rate < 30 mL/min per 1.73 m², uncontrolled atrial fibrillation, current spironolactone therapy, and physician preference.

The patients took spironolactone for 5 days to assess tolerability. Then, the drug was stopped, and they were studied at baseline and after ≥ 6 months of spironolactone therapy added to standard treatment. Each patient underwent CMR followed by [¹¹C] acetate PET imaging within 2 hours and then completed a 6-minute walk test and the Minnesota Living with Heart Failure questionnaire.³² Patients took spironolactone 25 mg daily, uptitrated to 50 mg daily, if possible, for ≥ 6 months. Seven patients took 50 mg, and 5 took 25 mg, averaging 39.6 mg among the 12 patients. The doses of ACE-I or ARB drug and beta-blocker remained

constant. After ≥ 6 months, the above tests were repeated. This study was approved by the Vanderbilt University and Nashville Veterans Affairs Institutional Review Boards, and all patients provided written informed consent.

PET Data Acquisition and Analysis

The patient lay supine in a hybrid PET/CT (computed tomography) scanner (GE Discovery STE; GE Health Care, Waukesha, WI). The heart rate (HR) and systemic blood pressure were recorded at baseline and every 5 minutes during data acquisition. A low-dose CT scan was obtained for attenuation correction, followed by intravenous bolus administration of [¹¹C] acetate (0.286 mCi/Kg). ECG-gated list mode images were acquired and processed as previously described, and the LV oxidative metabolic rate, k_{mono} , was determined by least squares fitting of the linear portion of the time-activity curve.²¹ The HR and arterial blood pressure were averaged during data acquisition.

The rate-pressure product (RPP) was calculated as $\text{HR} \times \text{systolic blood pressure}$ (beats per minute \times mm Hg). $k_{\text{mono}}/\text{RPP}$ was calculated as an index of energy supply to demand. The work metabolic index (WMI), a measurement of LV efficiency, was calculated as: $(\text{LVSVI} \times \text{SBP} \times \text{HR})/k_{\text{mono}}$, where LVSVI is LV stroke volume index (stroke volume/m²).¹⁶

CMR

CMR was performed using a commercially available 1.5-T Siemens Magnetom Avanto scanner (Siemens AG, Erlangen, Germany). Patients were scanned using a phased-array torso receiver coil. The imaging protocol consisted of 3 parts: cine imaging for ventricular volume and function; contrast-enhanced first-pass imaging for myocardial perfusion; and myocardial late gadolinium enhancement imaging. Following localizer images to identify the location of the heart within the thorax, cine imaging was first performed aligned to the horizontal and vertical long axis of the heart, from which a stack of contiguous short-axis cine images of the LV were acquired. Typical acquisition parameters for cine images were: field of view (FOV) 300 \times 340 mm; matrix 156 \times 192; slice thickness (SL) 8 mm; flip angle (FA) 80 degrees and adjusted downward depending on the specific absorption rate; echo time (TE) 1.1 ms; bandwidth (BW) 930 Hz/pixel; and usually 30 phases per cardiac cycle to maintain repetition time (TR) below 50 ms. Parallel imaging was employed using the generalized autocalibrating partially parallel acquisition (GRAPPA) technique with an acceleration factor of 2. The typical scan time was < 15 seconds per slice. After cine imaging, myocardial perfusion imaging was performed during the peak hyperemic effect of adenosine and under resting conditions. Adenosine (140 $\mu\text{g}/\text{kg}/\text{min}$) was infused

intravenously over 4 to 6 minutes. At 4 minutes into the adenosine infusion, 0.1 mmol/kg gadolinium-diethylenetriamine pentaacetic acid (Gd-DTPA; Magnevist, Bayer Health-Care Pharmaceuticals, Wayne, IN) was injected intravenously. First-pass imaging of the wash-in of Gd-DTPA through the LV myocardium was performed in 3 short-axis imaging planes positioned in mid-myocardial segments of the LV using a saturation-recovery turbo fast low angle shot gradient echo sequence. All 3 short-axis images were acquired with each R-R interval over 50 consecutive heart beats starting with the injection of Gd-DTPA in order to capture the initial wash-in of Gd-DTPA through the myocardium. Typical acquisition parameters for first-pass images were: FOV 320 × 400 mm; matrix 116 × 192; SL 8 mm; slice gap 8 mm; FA 12 degrees; TE 1.1 ms; TR 160 to 190 ms; BW 930 Hz/pixel; and GRAPPA acceleration factor 2. After a 5-minute delay, contrast-enhanced first-pass imaging was repeated under resting conditions with a second intravenous injection of 0.1 mmol/kg of Gd-DTPA (total combined dose, 0.2 mmol/kg of Gd-DTPA). Ten minutes after the initial injection of Gd-DTPA, short-axis myocardial late gadolinium enhancement imaging was performed using both single-shot inversion recovery (IR) and phase-sensitive inversion recovery (PSIR) true fast imaging with steady-state precession imaging. Typical acquisition parameters for first-pass images were: FOV 270 × 360 mm; matrix 108 × 192; SL 8 mm; FA 50 degrees; TE 1.1 ms; TR 700 ms; and BW 1200 Hz/pixel. IR and PSIR images were acquired every other cardiac cycle. To properly select the optimal inversion time (TI) delay, a TI “scout” sequence acquired at the 10-minute mark in a single short-axis imaging plane using the above parameters and with progressively longer TI times. The optimal TI was visually determined as the time delay when the myocardium appeared darkest. The average TI for IR imaging was 220 to 280 ms. PSIR imaging is less sensitive to TI, and the TI was set to 300 ms for all PSIR acquisitions.

The LV end diastolic volume, end systolic volume, stroke volume, LVEF, LV mass and mass index ([g]/body surface area [m²]), and RPP were calculated using standard equations, and LV mean systolic WS was calculated as shown here using a previously described method³³:

$$WS = \frac{P}{\left[\frac{V_{lum} + V_{myo}}{V_{lum}} \right]^{2/3}} - 1$$

where V_{lum} is ventricular inner volume, V_{myo} is ventricular myocardial wall volume, and P is systolic arterial pressure.

The myocardial perfusion index (MPI) was quantitated using commercial software (CMR Tools; Cardiovascular Imaging Solutions, London, UK),¹⁵ as the maximum slope of the time-intensity curve of myocardial enhancement of Gd-DTPA according to the following equation:

$$MPI = \frac{\text{maximum slope (myocardium)}}{\text{maximum slope (LV cavity)}}$$

The subendocardial and -epicardial borders were manually drawn for each frame to avoid inclusion of LV blood pool. Each of 6 LV segments was divided into subendocardial and -epicardial regions. The MPI was calculated for the transmural myocardium, subendocardium, and subepicardium at rest and during adenosine infusion and specifically for the anterior segment, an optimal region resulting from the absence of artifact. The ratio of MPI during adenosine compared to rest was calculated as the myocardial perfusion reserve index (MPRI):

Table 1. Characteristics and Hemodynamics of NIDCM Patients at Baseline (N=12)

	Baseline Median (IQR) or %	N
Sex (female)	33%	12
Age, y	52 (45 to 54)	12
Medications		
Beta-blockers	100%	12
ACE-I/ARB	100%	12
Diuretics	100%	12
Body surface area, m ²	2.1 (1.9 to 2.3)	12
Creatinine, mg/dL	0.96 (0.84 to 1.25)	12
NYHA class		
Class 2	42%	5
Class 3	58%	7
Mean right atrial pressure, mm Hg	7 (6.5 to 9.5)	7
Systolic PAP, mm Hg	33 (30 to 46)	7
Diastolic PAP, mm Hg	19 (15 to 27)	7
Mean PAP, mm Hg	21 to 36)	7
PCWP, mm Hg	18 (10 to 26)	7
Cardiac output*, L/min	4.0 (3.6 to 5.5)	6
Cardiac index*, L/min per m ²	2.1 (1.8 to 3.5)	7
LVSP, mm Hg	103 (95 to 105)	7
LVEDP or PCWP, mm Hg	26 (14 to 28)	11
EF by contrast ventriculography, %)	24 (17 to 31)	9
Coronary angiography findings		
No significant coronary artery disease**		10

ACE-I indicates angiotensin-converting enzyme inhibitor; ARB, angiotensin receptor blocking drug; EF, ejection fraction; IQR, interquartile range; LVEDP, left ventricular end diastolic pressure; LVSP, left ventricular systolic pressure; NIDCM, nonischemic dilated cardiomyopathy; NYHA, New York Heart Association; PAP, pulmonary artery pressure; PCWP, pulmonary capillary wedge pressure.

*Cardiac output and index was measured using the thermal dilution method during right heart catheterization; **no lesions greater than 50% luminal diameter reduction in any vessel.

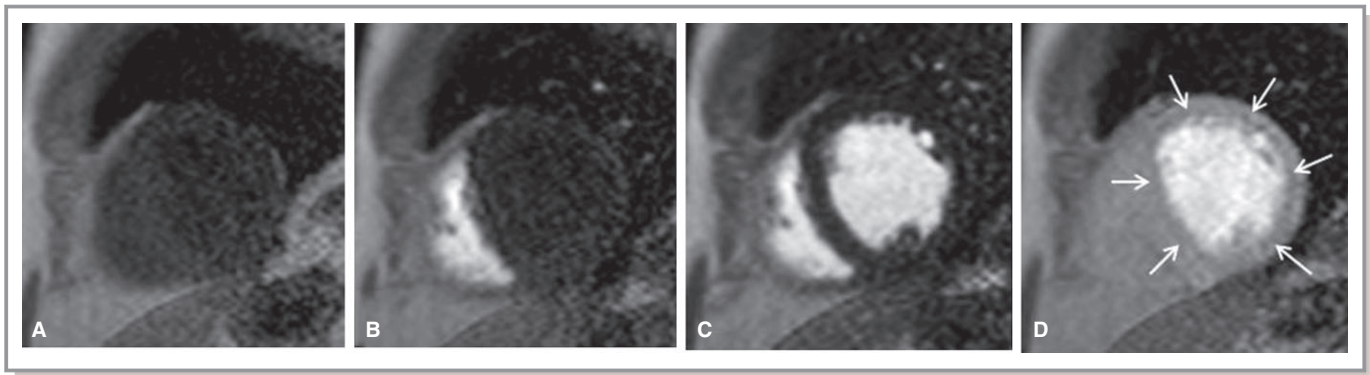


Figure 1. Selected mid-ventricular short-axis images during the first-pass transit of contrast through the heart. A, Before contrast arrival. B, Contrast arrival within the right ventricle. C, Contrast arrival within the left ventricle. D, Delayed endocardial contrast arrival (arrows).

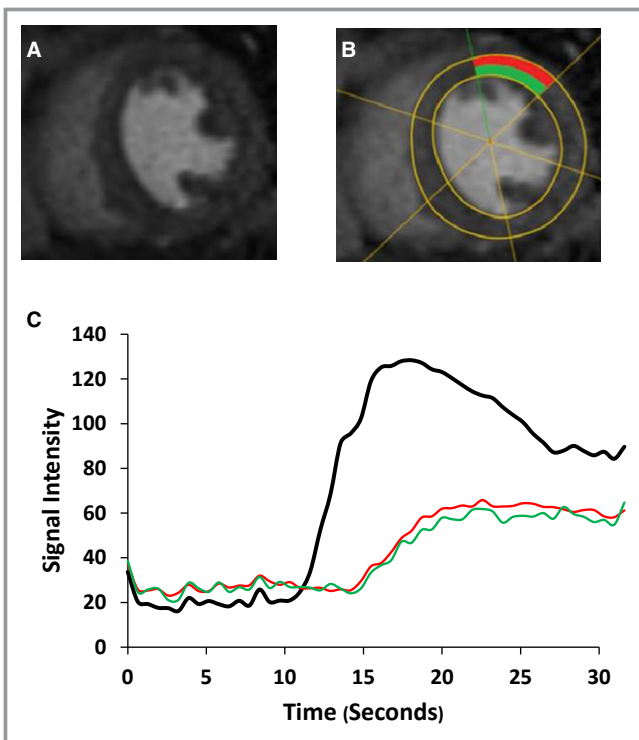


Figure 2. Mid-ventricular short-axis images of NIDCM patient. A, Peak arrival of Gd-DTPA within myocardium during adenosine infusion. B, LV segmented by software and anterior segment of mid-ventricular short-axis image selected for comparison, divided into endocardium (green) and epicardium (red). C, Signal intensity-time curves for LV (black), subendocardium, and subepicardium, as above. The LV curve shows earlier arrival and greater peak signal intensity than the myocardial segments. Gd-DTPA indicates gadolinium-diethylenetriamine pentaacetic acid; LV, left ventricular; NIDCM, nonischemic dilated cardiomyopathy.

$$MPRI = MPI(\text{adenosine})/MPI(\text{rest})$$

The reproducibility of acquiring contrast-enhanced first-pass imaging of gadolinium for MPI and MPRI was tested in 6 patients by repeating the CMR protocol on 2 separate days.

The transmural stress and rest MPI showed high reproducibility, with intraclass correlation coefficients of 0.96 and 0.99, respectively.

Statistical Analysis

We expressed the median and interquartile range (IQR) for continuous variables, and frequency and percentage for categorical variables. Before-and-after spironolactone comparisons used the Wilcoxon’s signed-rank test, with linear regression for correlation between k_{mono}/RPP and MPRI. All tests were 2 tailed with a significance level of 0.05. All analyses were performed using SPSS (version 18.0; SPSS, Inc., Chicago, IL) and the statistical programming language, R (version 2.15.1; R Development Core Team, Vienna, Austria).

Results

Twelve patients with NIDCM (8 males and 4 females) completed the study, with baseline characteristics shown in Table 1. The median age was 52 years, and all took both a beta-blocker and either an ACE-I or ARB drug. Before study entry, the median duration of taking any of these therapies was 21 weeks, and the median duration on stable doses of beta-blocker was 16 weeks. There was a median of 10 weeks (IQR, 6 to 16) between the initial clinical echocardiogram that met inclusion criteria and the baseline CMR study. Eleven patients had cardiac catheterization, with right heart hemodynamics in 7. The mean pulmonary capillary wedge or LV end diastolic pressures were elevated. The contrast ventriculographic LVEF was severely depressed, similar to the echocardiographic results. There was no significant coronary atherosclerosis in 10 of 10 catheterized patients, and the remaining 2 had no ischemia or infarction on nuclear stress perfusion imaging.

Table 2. CMR Measurements Before and After Spironolactone (N=12)

	Baseline Median (IQR)	After >6 Months of Spironolactone Median (IQR)	Mean Difference (SD)	P Value*
Ejection fraction, %	24 (16 to 28)	47 (41 to 53)	925 (10.2)	0.002
LV mass, g	169 (154 to 200)	150 (142 to 186)	14.3 (14.3)	0.005
LV mass index, g/m ²	83 (74.3 to 91.5)	73 (65.5 to 80.8)	7.7 (8.7)	0.002
LV wall stress, kPA	163 (147 to 186)	116 (100 to 137)	36.1 (40.1)	<0.001
LVEDV, mL	168 (146 to 191)	146 (131 to 170)	20.2 (13.7)	0.001
LVESV, mL	130 (115 to 163)	71 (66 to 106)	89.6 (42.5)	0.002
Stroke volume, mL	38 (28 to 47)	68 (60 to 82)	32.7 (18.3)	<0.001

CMR indicates cardiac magnetic resonance imaging; IQR, interquartile range; LV, left ventricular; LVEDV, LV end diastolic volume; LVESV, LV end systolic volume. *Wilcoxon’s signed-rank test.

The sequential appearance of contrast through a mid-ventricular short-axis slice after a venous contrast bolus injection is illustrated in Figure 1 (also, Video S1). Before contrast arrival, ventricular blood pool and myocardial signal are hypointense (Figure 1A). During the first-pass transit of contrast, contrast first appears within the right ventricle (Figure 1B), then the left ventricle (Figure 1C), and eventually within the myocardium (Figure 1D). Figure 1D further demonstrates a circumferential endocardial perfusion defect (arrows) that persists as the LV blood pool signal is fading. The perfusion defect is compatible with the concept of energy starvation and the quantitative abnormalities in MPI outlined below.

There was no late gadolinium myocardial enhancement consistent with macroscopic fibrosis or active myocarditis in

any of the participants’ images. Figure 2 shows the method of dividing the LV into 6 regions, with subendocardial and -epicardial halves, plus the signal intensity-time curves of Gd-DTPA in the LV blood pool and the anterior wall.

The baseline CMR data were consistent with NIDCM (Table 2). After ≥6 months of spironolactone therapy (median, 45 weeks; IQR, 27 to 74), CMR showed evidence for reverse remodeling, with significant reductions in LV mass index, LV wall stress, and LV end diastolic and end systolic volume, associated with an increase in stroke volume and LVEF (all $P \leq 0.002$). Before and after spironolactone, the median quality-of-life score improved from 54 (IQR, 26 to 71) to 22 (IQR, 20 to 44; $P=0.008$), and the 6-minute walk test distance increased from 521 m (IQR, 468 to 530) to 542 m (IQR, 523 to 604; $P=0.01$). There was no significant change in

Table 3. Hemodynamics During CMR at Rest and During Adenosine at Baseline and After Spironolactone (N=12)

	Baseline Median (IQR)	After >6 Months of Spironolactone Median (IQR)	Mean Difference (SD)	P Value*
Rest				
SBP, mm Hg	120 (115 to 124)	122 (114 to 131)	2 (11)	0.5
DBP, mm Hg	66 (64 to 72)	72 (66 to 77)	5 (9)	0.065
HR, beats/min	67 (58 to 71)	72 (65 to 75)	6 (7)	0.023
RPP, beats/min per mm Hg	8235 (6683 to 8542)	9080 (7936 to 9644)	892 (1141)	0.021
Adenosine				
SBP, mm Hg	124 (116 to 128)	124 (114 to 140)	4 (15)	0.48
DBP, mm Hg	68 (61 to 74)	70 (68 to 83)	7 (10)	0.023
HR, beats/min	84 (80 to 93)	86 (80 to 96)	4 (12)	0.25
RPP, beats min/mm Hg	9963 (9248 to 11 244)	11 592 (9758 to 12 570)	945 (2220)	0.129
Change in RPP from rest to adenosine, beats/min per mm Hg	1980 (1399 to 2659)	2460 (1633 to 3104)	53 (2263)	0.301

DBP indicates diastolic blood pressure; HR, heart rate; IQR, interquartile range; RPP, rate pressure product (systolic blood pressure×heart rate); SBP, systolic blood pressure. *Wilcoxon’s signed-rank test.

median nT-proBNP (608 vs. 508 pg/mL; $P=0.158$), creatinine (1.00 vs. 0.96 mg/dL; $P=0.48$), body mass index (31 vs. 31 kg/m²) or weight (91 vs. 91.5 kg) from baseline to follow-up. There was a small increase in blood urea nitrogen from a median of 12 mg/dL at baseline to 16 mg/dL at follow-up ($P=0.031$). Table 3 shows the hemodynamics during CMR at baseline and after spironolactone. After spironolactone, the resting HR increased, causing a slight increase in the resting RPP. However, HR and RPP during adenosine were not different before and after treatment. There was also no significant difference in the increase in RPP during adenosine infusion at baseline versus 6 months.

At baseline, the transmural, subendocardial, and subepicardial MPI increased with adenosine (Table 4; all $P<0.001$). The transmural MPRI at baseline was 1.72, comparable to the results of PET studies in NIDCM⁹⁻¹¹; however, CMR was able to show relative subendocardial hypoperfusion with an MPRI of 1.63 (IQR, 1.47 to 1.72), as compared to 1.83 (IQR, 1.67 to 1.98) in the subepicardium ($P=0.008$).

After spironolactone, the transmural MPI during adenosine increased slightly, but significantly, from 0.13 to 0.14 ($P=0.012$). Importantly, the cause was an increase in the subendocardial MPI from 0.13 (IQR, 0.11 to 0.14) to 0.15 (IQR, 0.13 to 0.17; $P<0.001$; Figure 3). The subendocardial MPRI increased from 1.63 (IQR, 1.47 to 1.72) at baseline to 1.80 (IQR, 1.72 to 1.89) after 6 months ($P<0.001$; Figure 4A).

There were no significant changes in MPI at rest in the transmural, subendocardial, or subepicardial layers, or in the subepicardium during adenosine infusion.

Eleven of 12 patients completed both PET studies (Table 5). There was no significant difference in RPP between baseline and ≥ 6 months. The k_{mono} increased slightly from 0.041 per minute at baseline to 0.042 per minute after spironolactone, whereas $k_{\text{mono}}/\text{RPP}$ and WMI also increased sharply (each $P\leq 0.003$). The individual increases in WMI are shown in Figure 4B. In the anterior subendocardial layer shown in Figure 2, a region with fewest artifacts, there was a significant, positive relationship between $k_{\text{mono}}/\text{RPP}$, as an index of energy supply versus demand, and the MPRI both at baseline and after >6 months' treatment. The findings held true in all 6 subendocardial regions, except in 2 patients who had imaging artifacts inferiorly. At baseline, $k_{\text{mono}}/\text{RPP}=4.2 \times 10^{-6}+(2.7 \times 10^{-8}) \times \text{MPRI}$, $R=0.63$, $P=0.002$. After >6 months of treatment, $k_{\text{mono}}/\text{RPP}=3.1 \times 10^{-6}+(3.2 \times 10^{-8}) \times \text{MPRI}$, $R=0.60$, $P=0.038$.

Discussion

We combined CMR and [¹¹C] acetate PET imaging to study the hypothesis of energy starvation in patients with NIDCM. We found that: (1) Patients with NIDCM have decreased subendocardial perfusion reserve associated with impaired oxidative

Table 4. Myocardial Perfusion Index in NIDCM Before and After Spironolactone (N=12)

	Baseline Median (IQR)	After >6 Months of Spironolactone Median (IQR)	Mean Difference (SD)	P Value*
Transmural				
Rest	0.072 (0.069 to 0.079)	0.073 (0.071 to 0.080)	0.009 (0.002)	0.91
Adenosine infusion	0.13 (0.12 to 0.14)	0.14 (0.13 to 0.15)	0.008 (0.006)	0.012
P value	<0.001	<0.001		
Endocardium				
Rest	0.077 (0.066 to 0.094)	0.078 (0.067 to 0.096)	0.009 (0.003)	0.52
Adenosine infusion	0.13 (0.11 to 0.14)	0.15 (0.13 to 0.17)	0.019 (0.017)	<0.001
P value	<0.001	<0.001		
Epicardium				
Rest	0.075 (0.063 to 0.086)	0.076 (0.063 to 0.086)	0.001 (0.003)	0.092
Adenosine infusion	0.14 (0.11 to 0.16)	0.14 (0.11 to 0.16)	0.003 (0.006)	0.077
P value	<0.001	<0.001		
MPRI				
Transmural	1.72 (1.67 to 1.87)	1.80 (1.76 to 1.92)	0.078 (0.07)	0.005
Endocardium	1.63 (1.47 to 1.72)	1.80 (1.72 to 1.89)	0.19 (0.09)	<0.001
Epicardium	1.83 (1.67 to 1.98)	1.83 (1.69 to 2.00)	0.008 (0.02)	0.677

IQR indicates interquartile range; MPRI, myocardial perfusion reserve index; NIDCM, nonischemic dilated cardiomyopathy. *Wilcoxon signed-rank test.

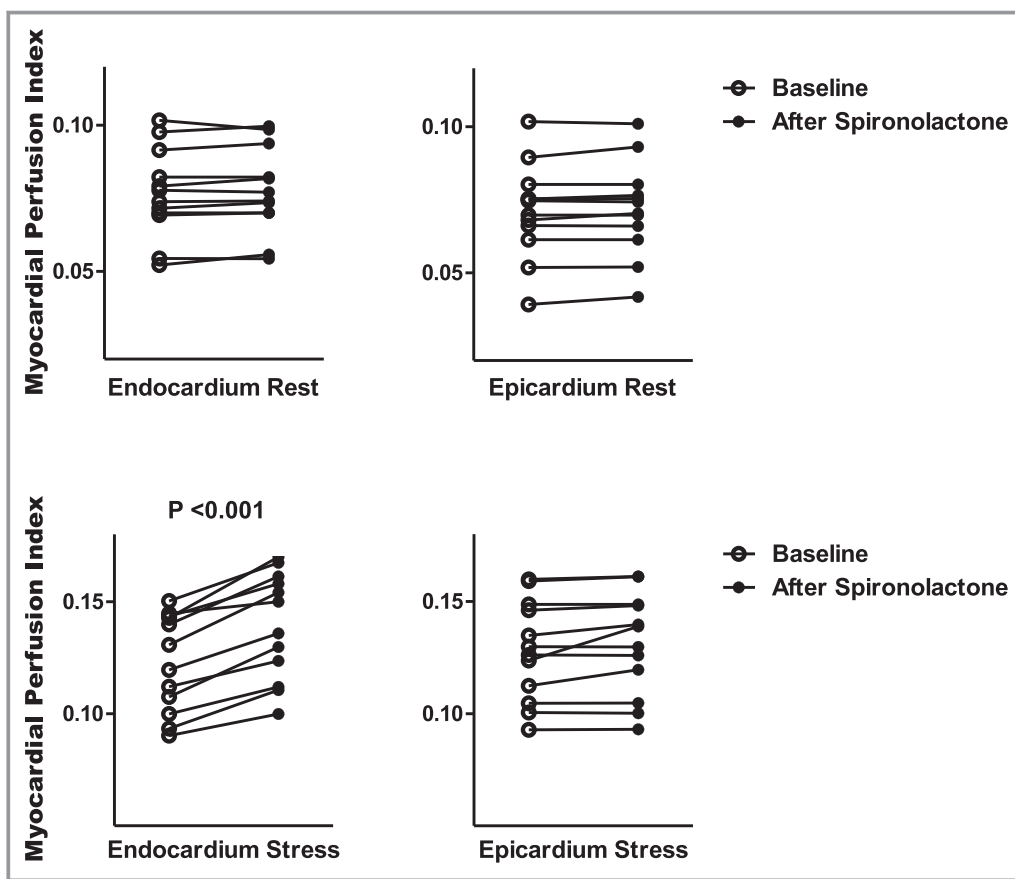


Figure 3. Comparison of myocardial perfusion index (MPI) in NIDCM at rest and during adenosine infusion for each subject at baseline and after ≥ 6 months of spironolactone therapy. NIDCM indicates nonischemic dilated cardiomyopathy.

metabolism versus demand and (2) aldosterone blockade plus standard HF therapy improved subendocardial perfusion and the supply-demand energy imbalance. These improvements were associated both with reverse LV remodeling and clinical improvements. To our knowledge, this is the first published work to use the superior resolution of CMR to differentiate subendocardial from transmural myocardial perfusion in patients with NIDCM.

According to the energy starvation hypothesis, LVH, fibrosis, and probable subendocardial ischemia^{34–36} produce metabolic stress,^{1,2} leading to reduced contractility, progressive LV dysfunction, elevated LV end diastolic pressure and adverse molecular consequences.^{2,8} In this study, we found, at baseline, LVH, LV chamber dilatation, and excess LV WS, consistent with HF. There was no visible late gadolinium enhancement (that would be consistent with fibrosis), suggesting that participants were relatively early in the disease process. This finding may be partly responsible for the consistently good response to antifailure therapy observed. After ≥ 6 months of spironolactone, there was significant reverse remodeling, with reduction in LV volumes,

LV mass index and WS, plus increased LV stroke volume and LVEF.

At baseline, there was relative subendocardial hypoperfusion and a blunted subendocardial MPRI, compared to the epicardium. This attenuated hyperemic response may be related to reports of endothelial dysfunction preceding the onset of HF in dogs,³⁷ microvascular remodeling in rats,³⁸ fibrosis with severe impairment of subendocardial perfusion reserve in a canine HF model,^{34,35,39} and impaired dilation of coronary microvasculature in patients.^{40,41} After spironolactone, we found marked improvement in the subendocardial MPI during hyperemia, an improved MPRI, and significant reverse remodeling. Such an improvement in perfusion could be the cause of the hemodynamic and clinical benefits in these patients.

LV efficiency measured by WMI improves in patients with HF treated with beta-adrenergic-blocking drugs⁴² and exercise training.¹¹ We found an increase in WMI of 58% after spironolactone plus a standard HF regimen, predominantly from a marked 79% increase in stroke volume (Tables 2 and 3), a greater percentage improvement in WMI than previously

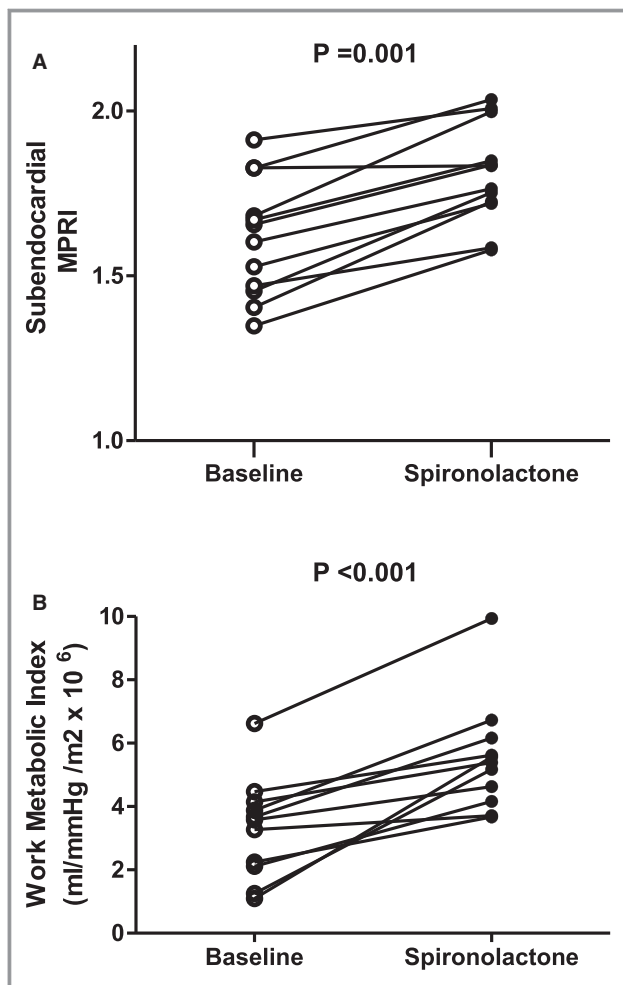


Figure 4. Comparison of subendocardial MPRI (A) and WMI (B) for each subject at baseline and after spironolactone therapy. The MPRI and WMI increased in 11 of 12 patients and decreased in none. MPRI indicates myocardial perfusion reserve index; WMI, work metabolic index.

reported. We previously showed that oxidative metabolism was inadequate to meet oxygen demands in NIDCM versus healthy subjects.²¹ In the present study, patients with NIDCM at baseline had similar results to our previous work with median $k_{\text{mono}}/\text{RPP}$ 5.5×10^{-6} , mean 5.9×10^{-6} . Both $k_{\text{mono}}/\text{RPP}$ and WMI increase with spironolactone therapy, supporting both an improvement in LV oxygen supply-demand relations and LV efficiency. The small increase in k_{mono} with similar RPP (Table 5) may be interpreted as a reduction in LV anaerobic metabolism in NIDCM. De Marco et al. reported transcatheter lactate production in a portion of patients with NIDCM, consistent with anaerobic metabolism.⁴³

Last, the subendocardial vasodilator reserve (MPRI) showed a significant positive correlation with LV metabolic supply-demand relations shown by $k_{\text{mono}}/\text{RPP}$. We cannot solely attribute the marked improvement in WMI to the improvements in $k_{\text{mono}}/\text{RPP}$ and MPRI, but we believe these

to be contributory. Aldosterone increases collagen formation in cultured rat fibroblasts⁴⁴ and causes marked perivascular fibrosis in the intact rat heart.²³ Aldosterone blockade seems additive to the beneficial remodeling by standard antifailure drugs. In animal models, spironolactone added to enalapril reduces LV cavity area, and when added to metoprolol further reduces LV cavity area and collagen density.^{45,46} In studies of patients with NIDCM, aldosterone blockade is associated with beneficial LV remodeling^{31,47} and remodeling when markers of collagen turnover decrease.^{31,48} Such remodeling is associated with clinical improvements in patients with mild symptoms of HF,^{30,47} similar to our patients.

Despite class I recommendation for adding an aldosterone antagonist to therapies for stage C systolic HF, less than one third of eligible patients receive aldosterone blockade after hospitalization for HF.^{49,50} Our data and other earlier data^{30,31,47,48} support this recommendation.

Study Limitations

There are several possible limitations. (1) Our patients received stable doses of HF medications before adding spironolactone (ACE-I or ARB drug, median 14 weeks, beta-blocker 16 weeks, and on either therapy 21 weeks). We do not fully ascribe the total improvements to spironolactone alone, given that these medications may have a synergistic role. (2) We had no control group, but because of the nature of the repeated measures, the patients serve as their own control group. (3) The patients had relatively mild LV remodeling at study entry, but they had already been treated with ACE-I or ARB drug and beta-blocking therapies. (4) There were relatively few patients, but nevertheless, the results were highly statistically significant and physiologically plausible. Possibly, even greater effects on LV reverse remodeling and the energy supply-demand relations might have been found if the patients had been studied before any HF treatment. (5) The CMR software automatically divided the myocardium into subendocardial and -epicardial halves. Visibly, the rim of hypoperfusion is smaller than the software modeled, including some better-perfused myocardium in the subendocardial zone. Nevertheless, the perfusion results were significant and may underestimate the extent of the finding.

Conclusions

This combination of CMR and [¹³C] acetate PET imaging demonstrated perfusion and metabolic components of HF that were compatible with the hypothesis of energy starvation. After adding spironolactone to the standard HF regimen, these components of energy starvation improved and were also associated with clinical improvement.

Table 5. Metabolic and Myocardial Perfusion Indices During PET Before and After Spirolactone (N=11)

	Baseline Median (IQR)	After >6 Months of Spirolactone Median (IQR)	Mean Difference (SD)	P Value*
$K_{mono}, \text{min}^{-1}$	0.041 (0.038 to 0.043)	0.042 (0.038 to 0.048)	0.002 (0.002)	0.001
RPP	6660 (5858 to 7930)	6778 (5912 to 7837)	30.5 (147)	0.424
$K_{mono}/RPP (\times 10^{-6}), \text{min}^{-1}/\text{beats min per mm Hg}$	5.5 (4.8 to 6.6)	6.4 (5.4 to 7.1)	0.3 (0.2)	0.003
Work metabolic index ($\times 10^6$), mL \times mm Hg/m ²	3.4 (2.2 to 3.9)	5.4 (4.4 to 5.9)	2.2 (1.3)	0.001

IQR indicates interquartile range; k_{mono} , monoexponential rate of [¹¹C] acetate clearance from left ventricular myocardium; NIDCM, nonischemic dilated cardiomyopathy; RPP, rate pressure product (systolic blood pressure \times heart rate).

*Wilcoxon's signed-rank test.

Acknowledgments

The authors thank Francesca Sabo, BS, Janine E. Belote, Sr, CNMT, RT (CT), Joseph Forrester, Sr, CNMT, RT (CT), Debra Rassel, RN, Linda Howerton, RN, Brenda White, RN, and Rebecca Hung, MD, for their contributions. The authors thank the Vanderbilt Heart Advisory Council Fund for their support. The Gd-DTPA was used off-label.

Sources of Funding

Supported, in part, by a Discovery Grant from the Vanderbilt University Medical Center and by the Vanderbilt National Center for Advancing Translational Sciences (grant UL1RR000445) National Institutes of Health (NIH)/National Center for Research Resources. Drs. Adkisson and Bell were supported by the NIH/National Heart, Lung and Blood Institute T32 HL07411-31. Dr. Bell is supported by K12 HD 043483-11 from the NIH/National Institute of Child Health and Human Development and the Eisenstein Women's Heart Fund.

Disclosures

None.

References

- Katz AM. Cardiomyopathy of overload. A major determinant of prognosis in congestive heart failure. *N Engl J Med.* 1990;322:100–110.
- Ingwall JS, Weiss RG. Is the failing heart energy starved? On using chemical energy to support cardiac function. *Circ Res.* 2004;95:135–145.
- Levy WC, Mozaffarian D, Linker DT, Sutradhar SC, Anker SD, Cropp AB, Anand I, Maggioni A, Burton P, Sullivan MD, Pitt B, Poole-Wilson PA, Mann DL, Packer M. The Seattle Heart Failure Model: prediction of survival in heart failure. *Circulation.* 2006;113:1424–1433.
- Katz AM. The myocardium in congestive heart failure. *Am J Cardiol.* 1989;63:12A–16A.
- Tsagalou EP, Anastasiou-Nana M, Agapitos E, Gika A, Drakos SG, Terrovitis JV, Ntalianis A, Nanas JN. Depressed coronary flow reserve is associated with decreased myocardial capillary density in patients with heart failure due to idiopathic dilated cardiomyopathy. *J Am Coll Cardiol.* 2008;52:1391–1398.
- Starling RC, Hammer DF, Altschuld RA. Human myocardial ATP content and in vivo contractile function. *Mol Cell Biochem.* 1998;180:171–177.
- Beer M, Seyfarth T, Sandstede J, Landschutz W, Lipke C, Kostler H, von Kienlin M, Harre K, Hahn D, Neubauer S. Absolute concentrations of high-energy phosphate metabolites in normal, hypertrophied, and failing human myocardium measured noninvasively with (31)P-SLOOP magnetic resonance spectroscopy. *J Am Coll Cardiol.* 2002;40:1267–1274.
- Neubauer S. The failing heart—an engine out of fuel. *N Engl J Med.* 2007;356:1140–1151.
- Neglia D, Michelassi C, Trivieri MG, Sambuceti G, Giorgetti A, Pratali L, Gallopin M, Salvadori P, Sorace O, Carpeggiani C, Poddighe R, L'Abbate A, Parodi O. Prognostic role of myocardial blood flow impairment in idiopathic left ventricular dysfunction. *Circulation.* 2002;105:186–193.
- Neglia D, Parodi O, Gallopin M, Sambuceti G, Giorgetti A, Pratali L, Salvadori P, Michelassi C, Lunardi M, Pelosi G. Myocardial blood flow response to pacing tachycardia and to dipyridamole infusion in patients with dilated cardiomyopathy without overt heart failure. A quantitative assessment by positron emission tomography. *Circulation.* 1995;92:796–804.
- Stolen KO, Kemppainen J, Ukkonen H, Kalliokoski KK, Luotolahti M, Lehikoinen P, Hamalainen H, Salo T, Airaksinen KE, Nuutila P, Knuuti J. Exercise training improves biventricular oxidative metabolism and left ventricular efficiency in patients with dilated cardiomyopathy. *J Am Coll Cardiol.* 2003;41:460–467.
- Wilke N, Simm C, Zhang J, Ellermann J, Ya X, Merkle H, Path G, Ludemann H, Bache RJ, Ugurbil K. Contrast-enhanced first pass myocardial perfusion imaging: correlation between myocardial blood flow in dogs at rest and during hyperemia. *Magn Reson Med.* 1993;29:485–497.
- Ugander M, Bagi PS, Oki AJ, Chen B, Hsu LY, Aletras AH, Shah S, Greiser A, Kellman P, Arai AE. Myocardial edema as detected by pre-contrast T1 and T2 CMR delineates area at risk associated with acute myocardial infarction. *JACC Cardiovasc Imaging.* 2012;5:596–603.
- Keijzer JT, van Rossum AC, Wilke N, van Eenige MJ, Jerosch-Herold M, Bronzwaer JG, Visser CA. Magnetic resonance imaging of myocardial perfusion in single-vessel coronary artery disease: implications for transmural assessment of myocardial perfusion. *J Cardiovasc Magn Reson.* 2000;2:189–200.
- Panting JR, Gatehouse PD, Yang GZ, Grothues F, Firmin DN, Collins P, Pennell DJ. Abnormal subendocardial perfusion in cardiac syndrome X detected by cardiovascular magnetic resonance imaging. *N Engl J Med.* 2002;346:1948–1953.
- Beanlands RS, Bach DS, Raylman R, Armstrong WF, Wilson V, Montieith M, Moore CK, Bates E, Schwaiger M. Acute effects of dobutamine on myocardial oxygen consumption and cardiac efficiency measured using carbon-11 acetate kinetics in patients with dilated cardiomyopathy. *J Am Coll Cardiol.* 1993;22:1389–1398.
- Armbrecht JJ, Buxton DB, Brunken RC, Phelps ME, Schelbert HR. Regional myocardial oxygen consumption determined noninvasively in humans with [1-11C]acetate and dynamic positron tomography. *Circulation.* 1989;80:863–872.
- Armbrecht JJ, Buxton DB, Schelbert HR. Validation of [1-11C]acetate as a tracer for noninvasive assessment of oxidative metabolism with positron emission tomography in normal, ischemic, posts ischemic, and hyperemic canine myocardium. *Circulation.* 1990;81:1594–1605.
- Brown M, Marshall DR, Sobel BE, Bergmann SR. Delineation of myocardial oxygen utilization with carbon-11-labeled acetate. *Circulation.* 1987;76:687–696.
- Brown MA, Myears DW, Bergmann SR. Validity of estimates of myocardial oxidative metabolism with carbon-11 acetate and positron emission tomography despite altered patterns of substrate utilization. *J Nucl Med.* 1989;30:187–193.
- Kronenberg MW, Cohen GI, Leonen MF, Mladi TA, Di Carli MF. Myocardial oxidative metabolic supply-demand relationships in patients with nonischemic dilated cardiomyopathy. *J Nucl Cardiol.* 2006;13:544–553.

22. Beanlands RS, Armstrong WF, Hicks RJ, Nicklas J, Moore C, Hutchins GD, Wolpers HG, Schwaiger M. The effects of afterload reduction on myocardial carbon 11-labeled acetate kinetics and noninvasively estimated mechanical efficiency in patients with dilated cardiomyopathy. *J Nucl Cardiol.* 1994;1:3–16.
23. Weber KT. Aldosterone in congestive heart failure. *N Engl J Med.* 2001;345:1689–1697.
24. Brilla CG, Pick R, Tan LB, Janicki JS, Weber KT. Remodeling of the rat right and left ventricles in experimental hypertension. *Circ Res.* 1990;67:1355–1364.
25. Weber KT, Pick R, Silver MA, Moe GW, Janicki JS, Zucker IH, Armstrong PW. Fibrillar collagen and remodeling of dilated canine left ventricle. *Circulation.* 1990;82:1387–1401.
26. Struthers AD, MacDonald TM. Review of aldosterone- and angiotensin ii-induced target organ damage and prevention. *Cardiovasc Res.* 2004;61:663–670.
27. Struthers AD. Aldosterone-induced vasculopathy: a new reversible cause of cardiac death. *J Renin Angiotensin Aldosterone Syst.* 2001;2:211–214.
28. Pitt B, Zannad F, Remme WJ, Cody R, Castaigne A, Perez A, Palensky J, Wittes J. The effect of spironolactone on morbidity and mortality in patients with severe heart failure. Randomized aldactone evaluation study investigators. *N Engl J Med.* 1999;341:709–717.
29. Pitt B, Remme W, Zannad F, Neaton J, Martinez F, Roniker B, Bittman R, Hurley S, Kleiman J, Gatlin M, Eplerenone Post-Acute Myocardial Infarction Heart Failure E, Survival Study I. Eplerenone, a selective aldosterone blocker, in patients with left ventricular dysfunction after myocardial infarction. *N Engl J Med.* 2003;348:1309–1321.
30. Zannad F, McMurray JJ, Krum H, van Veldhuisen DJ, Swedberg K, Shi H, Vincent J, Pocock SJ, Pitt B. Eplerenone in patients with systolic heart failure and mild symptoms. *N Engl J Med.* 2011;364:11–21.
31. Tsutamato T, Wada A, Maeda K, Mabuchi N, Hayashi M, Tsutsui T, Ohnishi M, Sawaki M, Fujii M, Matsumoto T, Matsui T, Kinoshita M. Effect of spironolactone on plasma brain natriuretic peptide and left ventricular remodeling in patients with congestive heart failure. *J Am Coll Cardiol.* 2001;37:1228–1233.
32. Rector TS, Kubo SH, Cohn JN. Validity of the minnesota living with heart failure questionnaire as a measure of therapeutic response to enalapril or placebo. *Am J Cardiol.* 1993;71:1106–1107.
33. Alter P, Rupp H, Rominger MB, Czerny F, Vollrath A, Klose KJ, Maisch B. A new method to assess ventricular wall stress in patients with heart failure and its relation to heart rate variability. *Int J Cardiol.* 2010;139:301–303.
34. Vatner SF, Shannon R, Hittinger L. Reduced subendocardial coronary reserve. A potential mechanism for impaired diastolic function in the hypertrophied and failing heart. *Circulation.* 1990;81:III8–III14.
35. Hittinger L, Shannon RP, Bishop SP, Gelpi RJ, Vatner SF. Subendomyocardial exhaustion of blood flow reserve and increased fibrosis in conscious dogs with heart failure. *Circ Res.* 1989;65:971–980.
36. Canetti M, Akhter MW, Lerman A, Karaal IS, Zell JA, Singh H, Mehra A, Elkayam U. Evaluation of myocardial blood flow reserve in patients with chronic congestive heart failure due to idiopathic dilated cardiomyopathy. *Am J Cardiol.* 2003;92:1246–1249.
37. Knecht M, Burkhoff D, Yi GH, Popilskis S, Homma S, Packer M, Wang J. Coronary endothelial dysfunction precedes heart failure and reduction of coronary reserve in awake dogs. *J Mol Cell Cardiol.* 1997;29:217–227.
38. Numaguchi K, Egashira K, Takemoto M, Kadokami T, Shimokawa H, Sueishi K, Takeshita A. Chronic inhibition of nitric oxide synthesis causes coronary microvascular remodeling in rats. *Hypertension.* 1995;26:957–962.
39. Vatner SF. Reduced subendocardial myocardial perfusion as one mechanism for congestive heart failure. *Am J Cardiol.* 1988;62:94E–98E.
40. Elkayam U, Khan S, Mehboob A, Ahsan N. Impaired endothelium-mediated vasodilation in heart failure: clinical evidence and the potential for therapy. *J Card Fail.* 2002;8:15–20.
41. Treasure CB, Vita JA, Cox DA, Fish RD, Gordon JB, Mudge GH, Colucci WS, Sutton MG, Selwyn AP, Alexander RW. Endothelium-dependent dilation of the coronary microvasculature is impaired in dilated cardiomyopathy. *Circulation.* 1990;81:772–779.
42. Beanlands RS, Nahmias C, Gordon E, Coates G, De Kemp R, Firnau G, Fallen E. The effects of beta(1)-blockade on oxidative metabolism and the metabolic cost of ventricular work in patients with left ventricular dysfunction: a double-blind, placebo-controlled, positron-emission tomography study. *Circulation.* 2000;102:2070–2075.
43. De Marco T, Chatterjee K, Rouleau JL, Parmley WW. Abnormal coronary hemodynamics and myocardial energetics in patients with chronic heart failure caused by ischemic heart disease and dilated cardiomyopathy. *Am Heart J.* 1988;115:809–815.
44. Brilla CG, Zhou G, Matsubara L, Weber KT. Collagen metabolism in cultured adult rat cardiac fibroblasts: response to angiotensin II and aldosterone. *J Mol Cell Cardiol.* 1994;26:809–820.
45. Goineau S, Pape D, Guillo P, Ramee MP, Bellissant E. Combined effects of enalapril and spironolactone in hamsters with dilated cardiomyopathy. *J Cardiovasc Pharmacol.* 2003;41:49–59.
46. Goineau S, Pape D, Guillo P, Ramee MP, Bellissant E. Combined effects of metoprolol and spironolactone in dilated cardiomyopathic hamsters. *J Cardiovasc Pharmacol.* 2002;40:543–553.
47. Chan AK, Sanderson JE, Wang T, Lam W, Yip G, Wang M, Lam YY, Zhang Y, Yeung L, Wu EB, Chan WW, Wong JT, So N, Yu CM. Aldosterone receptor antagonism induces reverse remodeling when added to angiotensin receptor blockade in chronic heart failure. *J Am Coll Cardiol.* 2007;50:591–596.
48. Udelson JE, Feldman AM, Greenberg B, Pitt B, Mukherjee R, Solomon HA, Konstam MA. Randomized, double-blind, multicenter, placebo-controlled study evaluating the effect of aldosterone antagonism with eplerenone on ventricular remodeling in patients with mild-to-moderate heart failure and left ventricular systolic dysfunction. *Circulation Heart Fail.* 2010;3:347–353.
49. Hunt SA, Abraham WT, Chin MH, Feldman AM, Francis GS, Ganiats TG, Jessup M, Konstam MA, Mancini DM, Michl K, Oates JA, Rahko PS, Silver MA, Stevenson LW, Yancy CW. 2009 Focused update incorporated into the ACC/AHA 2005 Guidelines for the Diagnosis and Management of Heart Failure in Adults: A Report of the American College of Cardiology Foundation/American Heart Association Task Force on Practice Guidelines: Developed in Collaboration with the International Society for Heart and Lung Transplantation. *Circulation.* 2009;119:e391–e479.
50. Albert NM, Yancy CW, Liang L, Zhao X, Hernandez AF, Peterson ED, Cannon CP, Fonarow GC. Use of aldosterone antagonists in heart failure. *JAMA.* 2009;302:1658–1665.